

## Synthesis and SAR of thiophene containing kinesin spindle protein (KSP) inhibitors

Anthony B. Pinkerton,<sup>a,\*</sup> Tom T. Lee,<sup>b</sup> Timothy Z. Hoffman,<sup>a</sup> Yan Wang,<sup>b</sup> Mehmet Kahraman,<sup>a</sup> Travis G. Cook,<sup>a</sup> Daniel Severance,<sup>a</sup> Timothy C. Gahman,<sup>a</sup> Stewart A. Noble,<sup>a</sup> Andrew K. Shiau<sup>b</sup> and Robert L. Davis<sup>b</sup>

<sup>a</sup>Department of Medicinal Chemistry, Kalypsys, Inc., 10420 Wateridge Circle, San Diego, CA 92121, USA

<sup>b</sup>Department of Biology, Kalypsys, Inc., 10420 Wateridge Circle, San Diego, CA 92121, USA

Received 21 March 2007; revised 18 April 2007; accepted 18 April 2007

Available online 29 April 2007

**Abstract**—We have identified and synthesized a series of thiophene containing inhibitors of kinesin spindle protein. SAR studies led to the synthesis of **33**, which was co-crystallized with KSP and determined to bind to an allosteric pocket previously described for other known KSP inhibitors.

© 2007 Elsevier Ltd. All rights reserved.

Anti-mitotic chemotherapeutics, such as the taxanes and vinca alkaloids, represent one of the main classes of effective cancer therapies, and are broadly used against a wide range of cancer types.<sup>1</sup> However, mechanism-related toxicities<sup>2</sup> and acquired resistance have stimulated considerable interest in developing anti-mitotics that target mechanisms other than direct microtubule inhibition. Kinesin spindle protein (KSP, also known as Eg5) is a member of a superfamily of force-generating motor proteins associated with microtubules.<sup>3a</sup> Like other kinesins, KSP contains a catalytic ATPase activity required for directed movement along microtubules. In dividing cells, the effects of KSP inhibition are limited to mitosis, while the only reported expression of KSP in non-dividing cells is in subsets of post-mitotic neurons, and its function there is unclear.<sup>3b</sup> Inhibition of KSP during mitosis leads to lack of formation or disruption of the bipolar mitotic spindle, sustained mitotic arrest, and subsequent induction of apoptosis both in vitro and in vivo.<sup>4</sup> Numerous small molecule inhibitors of the KSP ATPase have been recently described,<sup>5</sup> for example quinazolinone **1**,<sup>5i</sup> dihydropyrazole **2a**,<sup>5a</sup> and dihydropyrrole **2b**,<sup>5b</sup> and clinical trials have been initiated to validate KSP as a target for cancer therapeutics.<sup>6</sup>

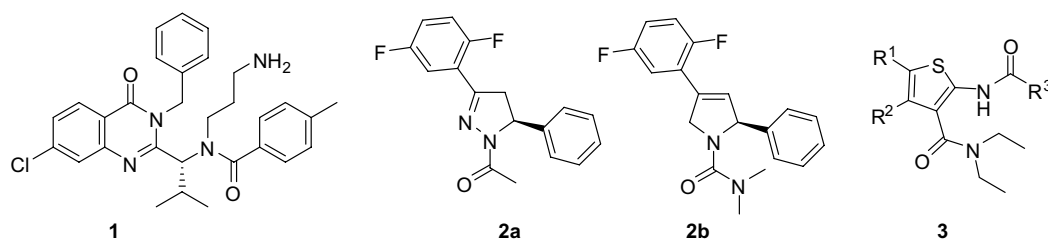
Ultra high-throughput screening of the Kalypsys compound collection identified a series of thiophene containing KSP inhibitors of the general structure **3**, with ATPase IC<sub>50</sub>s in the low micromolar range and effects on cultured cells consistent with selective targeting of KSP. Thus, a medicinal chemistry effort was initiated to optimize these screening hits and determine their mode of binding to KSP.

The compounds described herein were synthesized as outlined in Scheme 1.<sup>7</sup> Cyclic ketones **4** were reacted with ethyl cyanoacetate (**5**) and sulfur with a catalytic amount of morpholine in ethanol to give amino thiophenes **6** in moderate to good yields.<sup>8</sup> Ester hydrolysis followed by activation of the resulting acid with triphosgene and reaction with an amine afforded amino-thiophene amides **9**. Reductive amination of the pendant amine provided KSP inhibitors such as **10**. Additionally, **6** could be reacted with acid chlorides (**7**) to give amides **8** in moderate to excellent yields. Hydrolysis of the free acid and coupling to an amine gave KSP inhibitors of the general structure **11**.

To investigate the SAR and improve the potency three main areas were examined: (1) investigation of the pendant amide connected to the amino thiophene (N-linked), (2) substitution of the thiophene core, and (3) replacements of the diethylamide. Three in vitro assays were used to drive the SAR: (a) a biochemical assay that

**Keywords:** Eg5; KSP; Kinesin spindle protein; Anti-mitotics; Thiophenes.

\* Corresponding author. Tel.: +1 858 754 3457; fax: +1 858 754 3301; e-mail: [apinkerton@kalypsys.com](mailto:apinkerton@kalypsys.com)

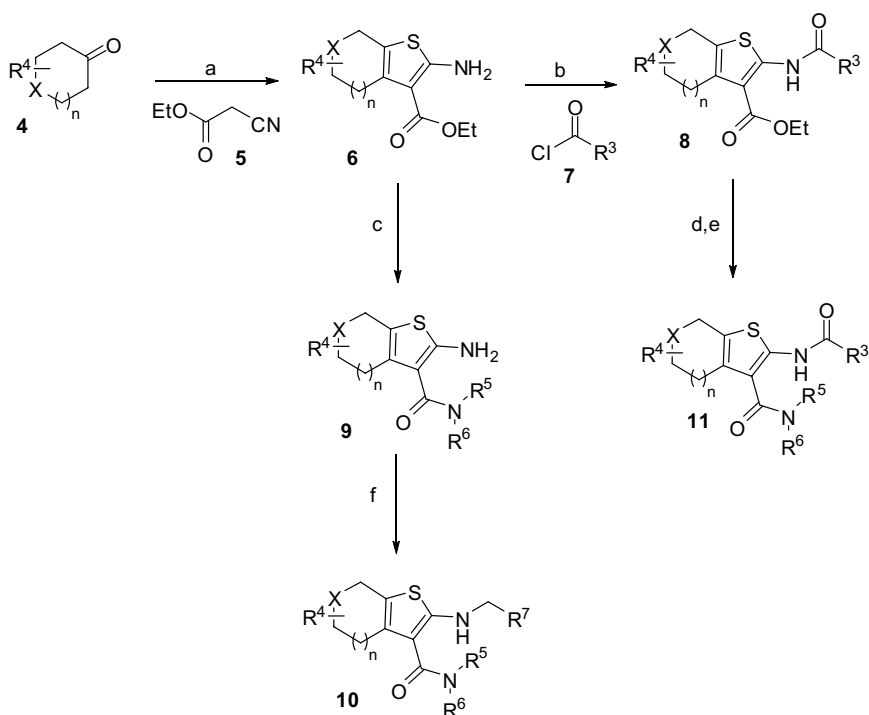


measures microtubule-stimulated KSP ATPase activity, (b) a cell-based assay that measures mitotic arrest maintained by KSP inhibition (MPM-2 cytoblot), and (c) a cell-based assay that measures cytotoxicity due to prolonged mitotic arrest, itself a result of continuous KSP inhibition.<sup>9–11</sup> In general, trends were consistent among the three assays.

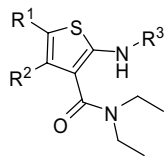
We initially examined substituent effects on the thiophene core as well as the effect of the pendant amide (Table 1). From the initial screen, a 2-thiophene amide at R<sup>3</sup> was found to be the most active analog (for example compound **14**), and thus was used as a starting point. As shown, only very weak activity was observed with an unsubstituted thiophene core (**12**). Some improvement was observed with dimethyl substitution (**13**), but more dramatic effects were observed with fused aliphatic rings appended onto the thiophene (**14–16**). In particular, cyclohexyl analog **15**, with activity in the ATPase assay of 1.7  $\mu$ M and the MPM-2 cytoblot assay of 0.48  $\mu$ M, became a scaffold for further optimization. Attempts to optimize the R<sup>3</sup> amide from the starting 2-thiophene were less successful, with the 3-thiophene (**17**), thiazole

(**18**), methyl thiazole (**19**), furan (**20**), and phenyl (**21**), all showing a log or more loss of activity. Removing the amide carbonyl of **15** to give amine derivative **22** also led to a log loss of activity. To further drive medicinal chemistry efforts, we determined the co-crystal structure of KSP with cyclohexyl analog **15**, Mg<sup>2+</sup>, and ADP to a resolution of 1.85  $\text{\AA}$ <sup>12</sup> (Fig. 1).

As shown in Figure 1A, compound **15** binds in a similar fashion to known KSP inhibitor **2b** at an allosteric site.<sup>5b</sup> The cyclohexylthiophene core of **15** occupies the same hydrophobic pocket as the difluorophenyl group of **2b**. One ethyl of the diethylamide group projects into solvent and the other in the pocket formed by Tyr211, Leu214, and Glu215. The pendant 2-thiophene amide of **15** fills the same pocket as the phenyl group of **2b**, leaving no extra space to accommodate any substituents on the thiophene ring. Using this information, we turned our focus to optimization of the diethylamide group. Initial exploration around the diethyl amide (Table 2) indicated that the hydrophobic interactions provided by amide substitution were required for activity. This conclusion is supported by the following observations:



**Scheme 1.** Reagents and conditions: (a) S, morpholine, EtOH, 50 °C, 40–95%; (b) Et<sub>3</sub>N, CH<sub>2</sub>Cl<sub>2</sub>, rt, 50–80%; (c) i—NaOH, EtOH, 70 °C, 72%; ii—triphosgene, THF, rt, quant.; iii—R<sup>5</sup>R<sup>6</sup>NH, DMF, 60 °C, 50–90%; (d) LiOH, THF/H<sub>2</sub>O, 1:1, 60 °C, 30–70%; (e) R<sup>5</sup>R<sup>6</sup>NH, HATU, DMF, rt, 20–60%; (f) R<sup>7</sup>CHO, NaBH(OAc)<sub>3</sub>, CH<sub>2</sub>Cl<sub>2</sub>, rt, 20–50%.

**Table 1.** Optimization of core and pendant amide

Compound	R <sup>1</sup>	R <sup>2</sup>	R <sup>3</sup>	ATPase IC <sub>50</sub> <sup>a</sup> (μM)	MPM-2 Cytoblot EC <sub>50</sub> <sup>a</sup> (μM)	Cytotoxicity 60 h EC <sub>50</sub> <sup>a</sup> (μM)
12	–H	–H		>100	NA <sup>b</sup>	NA <sup>b</sup>
13	–CH <sub>3</sub>	–CH <sub>3</sub>		23(5)	29(11)	>30
14	–(CH <sub>2</sub> ) <sub>3</sub> –			9.9(2.1)	2.2(0.2)	7.1(1.0)
15	–(CH <sub>2</sub> ) <sub>4</sub> –			1.7(0.4)	0.48(0.13)	2.0(0.2)
16	–(CH <sub>2</sub> ) <sub>5</sub> –			4.1(0.9)	5.8(6.8)	13(5)
17	–(CH <sub>2</sub> ) <sub>4</sub> –			13(2)	4.3(0.8)	29.4(0.1)
18	–(CH <sub>2</sub> ) <sub>4</sub> –			76(19)	>30	NA <sup>b</sup>
19	–(CH <sub>2</sub> ) <sub>4</sub> –			17(4)	>30	>30
20	–(CH <sub>2</sub> ) <sub>4</sub> –			23(5)	20(7)	>30
21	–(CH <sub>2</sub> ) <sub>4</sub> –			33(9)	34(18)	>30
22	–(CH <sub>2</sub> ) <sub>4</sub> –			20(8)	>30	>30

<sup>a</sup> Value represents the mean of three experiments with standard deviations shown in parentheses.

<sup>b</sup> NA, not active <30 μM.

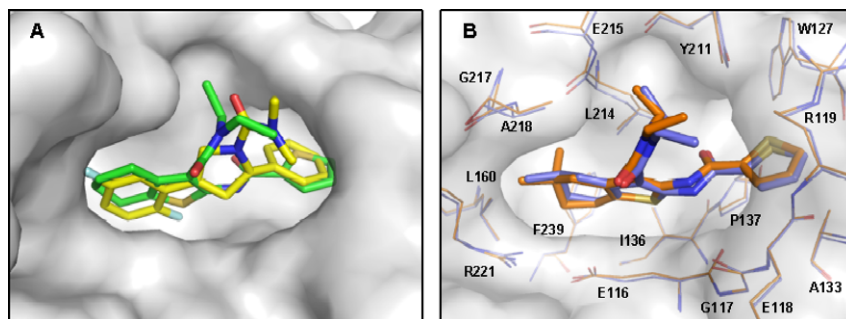
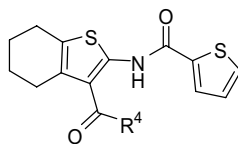


**Figure 1.** X-ray structures of compounds in the KSP allosteric binding site. (A) **2b** (yellow, PDB code 2FL6) and **15** (green, PDB code 2PG2); (B) **33** (blue, PDB code 2UYI) and **37** (orange, PDB code 2UYM). Protein surface is shown for KSP/ADP/15 (A) and KSP/ADP/33 (B). Compounds are shown in thick sticks, and protein residues are shown in thin sticks.

Table 2. Effect of amide substitution



Compound	R <sup>4</sup>	ATPase IC <sub>50</sub> <sup>a</sup> (μM)	MPM-2 Cytoblot EC <sub>50</sub> <sup>a</sup> (μM)	Cytotoxicity 60 h EC <sub>50</sub> <sup>a</sup> (μM)
23		>100	NA <sup>b</sup>	NA <sup>b</sup>
24		>100	NA <sup>b</sup>	NA <sup>b</sup>
25		>100	NA <sup>b</sup>	NA <sup>b</sup>
15		1.7(0.4)	0.48(0.13)	2.0(0.2)
26		6.0(1.6)	3.6(1.2)	12(2)
27		3.9(0.8)	1.1(0.1)	3.1(1.6)
28		2.8(0.7)	0.54(0.30)	5.1(2.2)
29		4.3(0.9)	1.8(0.4)	7.2(2.7)
30		27(6)	37(29)	>30
31		8.6(1.8)	7.6(1.4)	>30

<sup>a</sup> Value represents the mean of three experiments with standard deviations shown in parentheses.

<sup>b</sup> NA, not active <30 μM.

first, an unsubstituted amide abolished activity (**25**). Second, unbranched amide substitution, which has fewer conformations allowing contact (**30**), was less potent than a fully branched substitution (**31**). The fact that the ester (**23**) and acid (**24**) are inactive is consistent with this notion. Third, cyclization of the branched amide (**27–29**) gave comparable activity. Finally, the dimethylamide **26**, reduced in size, showed diminished potency.

Lastly we turned our attention to further optimization of the thiophene core (Table 3). From the crystal structure of **15**, we surmised that there was additional space in the hydrophobic pocket occupied by the cyclohexyl ring, in particular space occupied by the halogens in **1** and **2a/2b**. To test this hypothesis we added alkyl groups to various positions on the cyclohexyl ring to potentially enhance favorable hydrophobic interactions. These and other substituted cycloalkylthiophene compounds were synthesized and tested as racemic mixtures unless otherwise noted. Satisfyingly, we found that a methyl group in the 2 position (**33**) gave a three- to fourfold boost in potency over **15** in both the ATPase assay (0.48 μM

vs 1.7 μM) and the MPM-2 cyto blot assay (0.10 μM vs 0.48 μM). Co-crystallization of **33** showed that the methyl group occupied an additional part of the main hydrophobic pocket (Fig. 1B). In addition, **33** was resolved into its enantiomers and one isomer was found to be 10 fold more active than the other.<sup>15</sup> Addition of another methyl group at position 2 (**37**) of the cyclohexylthiophene was tolerated but led to a loss of activity compared to **15**. An X-ray structure shows that the axial methyl group in **37** makes close contact (3.2 Å) to the polar main chain oxygen of Leu214 as shown in Figure 1B. Furthermore, the Cα atoms of 213–218 move an average of 0.34 Å away from **37**, resulting in slight opening of the pocket as compared to **33**. Attempts to increase the size beyond methyl, as in **39**, were detrimental. Substitutions at other positions of the cyclohexylthiophene were less favorable than position 2 (compare **33** to **32**, or **34**; **37** to **38**; or **39** to **40**). An energy penalty likely occurs by rearranging adjacent residues in order to avoid close contacts incurred by these substitutions. A similar boost in potency was observed when a methyl group was incorporated on the cyclohexyl-

Table 3. Core optimization

Compound	CORE	ATPase IC <sub>50</sub> <sup>a</sup> (μM)	MPM-2 Cytoblot EC <sub>50</sub> <sup>a</sup> (μM)	Cytotoxicity 60 h EC <sub>50</sub> <sup>a</sup> (μM)
32(1)		7.5(1.6)	4.7(1.4)	6.3(1.7)
33(2)		0.48(0.11)	0.10(0.03)	1.0(0.7)
34(3)		5.9(1.1)	2.6(1.0)	6.1(0.9)
35(1)		8.1(1.0)	5.4(1.9)	36(19)
36(2)		3.5(0.6)	1.5(0.4)	7.7(4.9)
37		3.1(0.9)	1.7(0.8)	6.0(2.6)
38		12(1)	14(7)	24(4)
39(2)		7.4(1.0)	1.9(0.4)	12(2)
40(3)		69(1)	>30	7.3(1.2)
41		24(4)	17(5)	>30
42		3.3(0.9)	9.6(9.5)	>30
43		>100	NA <sup>b</sup>	NA <sup>b</sup>
44		>100	NA <sup>b</sup>	NA <sup>b</sup>

<sup>a</sup> Value represents the mean of three experiments with standard deviations shown in parentheses.

<sup>b</sup> NA, not active <30 μM.

tyl analog, for example activity was improved to 3.5 μM (for **36**) from 9.9 μM (for **14**) in the ATPase assay. Attempts to incorporate heteroatoms into the ring led to a range of results, from a minor effect for sulfur (**42**), to a detrimental effect with oxygen (**41**) and complete loss of activity with nitrogen (**43**). This suggests that polar substituents are not tolerated in the hydrophobic pocket.<sup>5a</sup> Somewhat surprisingly, benzothiophene analog **44** showed no activity, although subsequent modeling into the active site indicated that the aromatic ring was not as well tolerated. Naphthalene and benzofuran analogs also showed no activity (data not shown).

To confirm that the cytotoxic activity was a consequence of KSP inhibition, we further characterized the cellular activity of compounds **15** and **33** (Fig. 2). Non-synchronously dividing A-549 lung cancer cells were treated for 18 h with vehicle alone (A), compound **33** (B), or compound **15** (not shown). Incubation with compound **33** or **15** resulted in the accumulation of cells with the typical monopolar spindle morphology due to KSP inhibi-

tion. No additional effect on cell morphology prior to induction of apoptosis was observed.

Flow cytometry of non-synchronous A-549 cells treated for 18 h with 15 μM compound **15** demonstrated a majority with a 4 N (G2/M) DNA content, consistent with mitotic arrest. For comparison, compounds **1**, and **2a** (as a racemic mixture), generated a similar profile at 1 μM (Table 4A). Cells previously treated for 18 h were washed and cultured for an additional 24 h in the absence of compounds (Table 4B). In this case, the effect of previous compound **15** treatment was mostly reversible, as was the case for compound **2a**. By contrast, the effect of previous compound **1** treatment was not reversible, with most cells continuing to have a 4 N DNA content, and some increase in the sub-2 N fraction associated with apoptotic and dead cells.

A-549 cells have been reported to aberrantly exit mitosis after prolonged mitotic arrest due to KSP inhibition by treatment with 200 μM monastrol. However, this exit

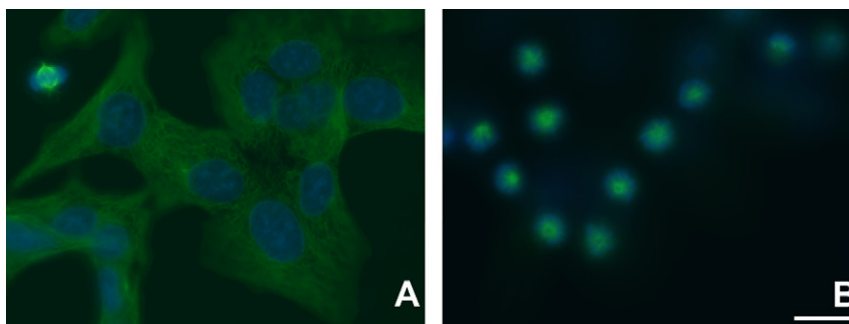


**Figure 2.** Imaging of cells following treatment with DMSO vehicle (A) or 10  $\mu\text{M}$  compound **33** (B).<sup>16</sup> Separate images of microtubules (green) and DNA (blue) are overlaid. (A) shows a single normal mitosis in the upper left, while (B) shows numerous cells with the monopolar spindle phenotype. Scale bar = 20  $\mu\text{m}$ .

**Table 4.** Flow cytometry of compound-treated A-549 cells

DNA content	<2 N	2 N	>2 N, <4 N	4 N
Cell cycle phase	Apoptotic	G <sub>1</sub>	S	G <sub>2</sub> /M
<b>A<sup>a</sup></b>				
DMSO	7	64	13	12
<b>1</b> , 1 $\mu\text{M}$	3	17	12	61
<b>2a</b> , 1 $\mu\text{M}$	2	14	11	64
<b>15</b> , 15 $\mu\text{M}$	3	18	14	56
<b>B<sup>b</sup></b>				
DMSO	0.5	58	17	16
<b>1</b> , 1 $\mu\text{M}$	10	8	7	64
<b>2a</b> , 1 $\mu\text{M}$	5	46	14	24
<b>15</b> , 15 $\mu\text{M}$	4	47	12	25

<sup>a</sup> Cells were treated for 18 h with DMSO vehicle or the listed compounds and processed for flow cytometry.<sup>17</sup> Table values are expressed as percentages. The remaining percentage of the sample is in multi-cell aggregates and not listed.

<sup>b</sup> Cells were treated for 18 h with DMSO vehicle or the listed compounds then washed and cultured in the absence of compounds for an additional 24 h before processing for flow cytometry.<sup>17</sup> Table values are expressed as percentages. The remaining percentage of the sample is in multi-cell aggregates and not listed.

does not occur until at least 36 h of continuous arrest, and is followed by a G<sub>1</sub>-like arrest with a 4 N DNA content.<sup>18</sup> Our results suggest shorter periods of mitotic arrest are insufficient for A-549 cells to commit to mitotic slippage, at least for compounds **15** and **2a**. Finally, the cell viability assay was used to demonstrate that significant apoptosis does not begin until at least 24 h after incubation of compounds **15** or **33**, consistent with other KSP inhibitors.<sup>19</sup>

In conclusion, a new class of thiophene containing compounds that are inhibitors of KSP have been developed from a uHTS screening lead. These compounds have been shown to have sub-micromolar activity in secondary cellular assays and a cell phenotype consistent with KSP inhibition. Structural information gained from co-crystal structures with KSP should help in the further development of these and other structural classes of KSP inhibitors.

## References and notes

- Dutcher, J. P.; Novik, Y.; O'Boyle, K.; Marcoullis, G.; Secco, C.; Wiernik, P. H. *J. Clin. Pharmacol.* **2000**, *40*, 1097.
- Quasthoff, S.; Hartung, H. P. *J. Neurol.* **2002**, *249*, 9.
- (a) Wood, K. W.; Cornwell, W. D.; Jackson, J. R. *Curr. Opin. Pharmacol.* **2001**, *1*, 370; (b) Ferhat, L.; Cook, C.; Chauviere, M.; Harper, M.; Kress, M.; Lyons, G. E.; Baas, P. W. *J. Neurosci.* **1998**, *18*, 7822.
- (a) Mayer, T. U.; Kapoor, T. M.; Haggarty, S. J.; King, R. W.; Schreiber, S. L.; Mitchison, T. J. *Science* **1999**, *286*, 971; (b) Sakowicz, R.; Finer, J. T.; Beraud, C.; Crompton, A.; Lewis, E.; Fritsch, A.; Lee, Y.; Mak, J.; Moody, R.; Turincio, R.; Chabala, J. C.; Gonzales, P.; Roth, S.; Weitman, S.; Wood, K. W. *Cancer Res.* **2004**, *64*, 3276; (c) Heald, R. *Cell* **2000**, *102*, 399; (d) Sharp, D. J.; Rogers, G. C.; Scholey, J. M. *Nature* **2000**, *407*, 41; (e) Mandelkow, E.; Mandelkow, E.-M. *Trends Cell Biol.* **2002**, *12*, 585; (f) Endow, S. A.; Barker, D. S. *Annu. Rev. Physiol.* **2003**, *65*, 161; (g) Sarli, V.; Giannis, A. *Chem. Med. Chem.* **2006**, *1*, 293.
- (a) Cox, C. D.; Breslin, M. J.; Mariano, B. J.; Coleman, P. J.; Buser, C. A.; Walsh, E. S.; Hamilton, K.; Huber, H. E.; Kohl, N. E.; Torrent, M.; Yan, Y.; Kuo, L. C.; Hartman, G. D. *Bioorg. Med. Chem. Lett.* **2005**, *15*, 2041; (b) Fraley, M. E.; Garbaccio, R. M.; Arrington, K. L.; Hoffman, W. F.; Tasber, E. S.; Coleman, P. J.; Buser, C. A.; Walsh, E. S.; Hamilton, K.; Fernandes, C.; Schaber, M. D.; Lobell, R. B.; Tao, W.; South, V. J.; Yan, Y.; Kuo, L. C.; Prueksaritanont, T.; Shu, C.; Torrent, M.; Heimbrook, D. C.; Kohl, N. E.; Huber, H. E.; Hartman, G. D. *Bioorg. Med. Chem. Lett.* **2006**, *16*, 1775; (c) Garbaccio, R. M.; Fraley, M. E.; Tasber, E. S.; Olson, C. M.; Hoffman, W.

- F.; Arrington, K. L.; Torrent, M.; Buser, C. A.; Walsh, E. S.; Hamilton, K.; Schaber, M. D.; Fernandes, C.; Lobell, R. B.; Tao, W.; South, V. J.; Yan, Y.; Kuo, L. C.; Prueksaritanont, T.; Slaughter, D. E.; Shu, C.; Heimbrook, D. C.; Kohl, N. E.; Huber, H. E.; Hartman, G. D. *Bioorg. Med. Chem. Lett.* **2006**, *16*, 1780; (d) Cox, C. D.; Torrent, M.; Breslin, M. J.; Mariano, B. J.; Whitman, D. B.; Coleman, P. J.; Buser, C. A.; Walsh, E. S.; Hamilton, K.; Schaber, M. D.; Lobell, R. B.; Tao, W.; South, V. J.; Kohl, N. E.; Yan, Y.; Kuo, L. C.; Prueksaritanont, T.; Slaughter, D. E.; Li, C.; Mahan, E.; Lu, B.; Hartman, G. D. *Bioorg. Med. Chem. Lett.* **2006**, *16*, 3175; (e) Tarby, C. M.; Kaltenbach, R. F., III; Huynh, T.; Pudzianowski, A.; Shen, H.; Ortega-Nanos, M.; Sheriff, S.; Newitt, J. A.; McDonnell, P. A.; Burford, N.; Fairchild, C. R.; Vaccaro, W.; Chen, Z.; Borzilleri, R. M.; Naglich, J.; Lombardo, L. J.; Gottardis, M.; Trainor, G. L.; Roussel, D. L. *Bioorg. Med. Chem. Lett.* **2006**, *16*, 2095; (f) Kim, K. S.; Lu, S.; Cornelius, L. A.; Lombardo, L. J.; Borzilleri, R. M.; Schroeder, G. M.; Sheng, C.; Rovnyak, G.; Crews, D.; Schmidt, R. J.; Williams, D. K.; Bhide, R. S.; Traeger, S. C.; McDonnell, P. A.; Mueller, L.; Sheriff, S.; Newitt, J. A.; Pudzianowski, A. T.; Yang, Z.; Wild, R.; Lee, F. Y.; Batorsky, R.; Ryder, J. S.; Ortega-Nanos, M.; Shen, H.; Gottardis, M.; Roussel, D. L. *Bioorg. Med. Chem. Lett.* **2006**, *16*, 3937; (g) Liu, F.; You, Q.-D.; Chen, Y.-D. *Bioorg. Med. Chem. Lett.* **2007**, *17*, 722; (h) Sunder-Plassmann, N.; Sarli, V.; Gartner, M.; Utz, M.; Seiler, J.; Huemmer, S.; Mayer, T. U.; Surrey, T.; Giannis, A. *Bioorg. Med. Chem.* **2005**, *13*, 6094; (i) Gartner, M.; Mueller, T.; Simon, J. C.; Giannis, A.; Sleeman, J. P. *Chem. Biol. Chem.* **2005**, *6*, 1; (j) Gartner, M.; Sunder-Plassmann, N.; Seiler, J.; Utz, M.; Vernos, I.; Surrey, T.; Giannis, A. *Chem. Biol. Chem.* **2005**, *6*, 1173; (k) Sarli, V.; Huemmer, S.; Sunder-Plassmann, N.; Mayer, T. U.; Giannis, A. *Chem. Biol. Chem.* **2005**, *6*, 2005; (l) Bergnes, G.; Brejc, K.; Belmont, L. *Curr. Top. Med. Chem.* **2005**, *5*, 127.
- (a) Duhl, D. M.; Renhowe, P. A. *Curr. Opin. Drug Discov. Dev.* **2005**, *8*, 431; (b) Coleman, P. J.; Fraley, M. E. *Expert Opin. Ther. Patents* **2004**, *14*, 1659; (c) Jackson, J. R.; Patrick, D. R.; Dar, M. M.; Huang, P. S. *Nat. Rev. Cancer* **2007**, *7*, 107.
  - All final compounds displayed spectral data (NMR, MS) that were consistent with the assigned structure.
  - Andersen, H. S.; Olsen, O. H.; Iversen, L. F.; Sorensen, A. L. P.; Mortensen, S. B.; Christensen, M. S.; Branner, S.; Hansen, T. K.; Lau, J. F.; Jeppesen, L.; Moran, E. J.; Su, J.; Bakir, F.; Judge, L.; Shahbaz, M.; Collins, T.; Vo, T.; Newman, M. J.; Ripka, W. C.; Moller, N. P. H. *J. Med. Chem.* **2002**, *45*, 4443.
  - Microtubule-stimulated KSP ATPase activity was determined by measuring production of ADP (ADPQuest Assay, DiscoverX). Affinity purified, catalytically active human KSP protein fragment (residues 1–386, C-terminal His<sub>6</sub>-tagged) in 20  $\mu$ l of assay buffer was dispensed to black 384-well assay plates. Compounds in DMSO and arrayed in 11 point 1/2 log dilution dose response (final top concentration of 96  $\mu$ M, 1% DMSO in all assay wells) were added by passive pin transfer, followed by addition of 5  $\mu$ l assay buffer containing taxol-stabilized bovine brain microtubules (Cytoskeleton) and ATP. The final concentrations of KSP, microtubules, and ATP were 15 nM, 500 nM, and 30  $\mu$ M, respectively. After a 2-h room-temperature incubation, ADPQuest assay reagents were added according to the manufacturer's instructions, and the resulting fluorescence signal was read on a Molecular Devices Acquest plate reader. Raw fluorescence data were normalized to negative (DMSO) and positive (compound **2a**, as a racemic mixture) controls. Data analysis was performed using Spotfire (v8.1, Spotfire, Inc.) and Kalypsys proprietary software.
  - Mitotic arrest maintained by KSP inhibition was assayed using A-549 human non-small cell lung carcinoma cells (CCL-185, ATCC). If A-549 cells synchronized in mitosis by nocodazole treatment are replated in the absence of nocodazole, ~100% of the cells will exit mitosis, and daughter cells will acquire a flat morphology within 4 h. However, if KSP is inhibited immediately after nocodazole washout, cells will remain in mitotic arrest, which can be demonstrated by measuring levels of the MPM-2 phospho-epitope<sup>13</sup>. Compounds in DMSO and arrayed in 11 point 1/2 log dilution dose response (final top concentration of 96  $\mu$ M, 1% DMSO in all assay wells) were added by passive pin transfer to culture medium (with 1% fetal bovine serum) previously dispensed to black 384-well assay plates. A-549 cells treated for 10 h with 1  $\mu$ M nocodazole were harvested, washed, and dispensed to the compound-pinned assay plates at  $3 \times 10^5$  cells/ml. Four hours later, cells were washed and fixed with 2% paraformaldehyde in phosphate-buffered saline for 10 min at room temperature. Fixed cells were then processed for a typical 'cytoblot' assay<sup>14</sup>, using MPM-2 primary antibody (Upstate Cell Signaling), donkey anti-mouse IgG (Fab<sub>2</sub>) horseradish peroxidase conjugate (Jackson ImmunoResearch), and a chemiluminescent substrate (POD, Roche Applied Science). Signal detection, data normalization, and data analysis were similar to that in Ref. 9.
  - A-549 cells were dispensed to white 384-well assay plates at  $1 \times 10^5$  cells/ml in medium with 1% fetal bovine serum. Compounds in DMSO and arrayed in 11 point 1/2 log dilution dose response (final top concentration of 96  $\mu$ M, 1% DMSO in all assay wells) were added by passive pin transfer. After 60 h incubation, cell viability was measured by dispensing an equal volume of ATPLite reagent (Perkin-Elmer). Signal detection, data normalization, and data analysis were similar to that in Ref. 9.
  - An N-terminal His<sub>6</sub>-tagged catalytically active fragment of KSP (1–368) was expressed in *Escherichia coli* and purified over a Ni-NTA column. The His<sub>6</sub> tag was removed, and the protein was further purified over a HiTrap Q column. Crystals were prepared at 4 °C using the hanging drop method. Protein [10 mg/mL in 50 mM Pipes (pH 6.8), 1 mM ATP, 2 mM MgCl<sub>2</sub>, 1 mM EGTA, and 1 mM Tris (2-carboxyethyl)phosphine hydrochloride] was mixed with 2 mM compound and incubated on ice for 1 h. The initial drop contained equal volumes of complex and well buffer [100 mM Bis-Tris (pH 6.0), 200 mM ammonium sulfate, and 18–20% PEG3350], and 10 mM SrCl<sub>2</sub> was also added to the drop. Crystallization was improved by microseeding, and the seeded drops were left at 4 °C for 2–3 days. Crystals were soaked in cryoprotecting solution (well buffer with PEG concentration increased to 35%) before freezing in liquid nitrogen. Data were collected at the Advanced Light Source beam line 5.0.2 (LBL). Structures were determined by molecular replacement using the KSP/ADP/monastol complex (PDB ID:1Q0B) as the search model. Crystallographic data are as follows. KSP/ADP/15: resolution = 1.85 Å, space group = C2,  $a = 161.1$  Å,  $b = 80.4$  Å,  $c = 69.3$  Å,  $\beta = 96.8^\circ$ ,  $R/R_{\text{free}} = 0.210/0.248$ ; KSP/ADP/33: resolution = 2.1 Å, space group = P2<sub>1</sub>2<sub>1</sub>2<sub>1</sub>,  $a = 69.5$  Å,  $b = 80.1$  Å,  $c = 159.0$  Å,  $R/R_{\text{free}} = 0.240/0.294$ ; KSP/ADP/37: resolution = 2.11 Å, space group = C2,  $a = 160.8$  Å,  $b = 80.5$  Å,  $c = 68.8$  Å,  $\beta = 96.2^\circ$ ,  $R/R_{\text{free}} = 0.208/0.272$ .
  - Davis, F. M.; Tsao, T. Y.; Fowler, S. K.; Rao, P. N. *Proc. Natl. Acad. Sci. U.S.A.* **1983**, *80*, 2926.
  - Stockwell, B. R.; Haggarty, S. J.; Schreiber, S. L. *Chem. Biol.* **1999**, *6*, 71.

15. Compound **33** was resolved using a Chiralpak IA column (4.6 mm × 250 mm) eluting 10% *i*-PrOH/90% heptane/0.1% TFA, 1 mL/min. The first eluting isomer showed ATPase activity of 0.48 μM versus 3.9 μM for the second eluting isomer. The absolute stereochemistry was not determined; the resolution of the crystal structure was not sufficient for definitive assignment.
16. A-549 cells were plated at  $1 \times 10^5$  cells/ml into glass coverslip chambers in medium with 1% fetal bovine serum. DMSO vehicle (1% final) alone or containing compounds (10 μM final) was added and cells incubated for 18 h. Cells were then washed and fixed with 100% ice-cold methanol for 10 min at room temperature. Fixed cells were processed for immunofluorescence microscopy of microtubules using anti-alpha tubulin mAb (DM1A, Sigma) and donkey anti-mouse IgG (Fab<sub>2</sub>) Alexa 488 (Invitrogen). Chromosomal DNA was stained with 4'-6-diamidino-2-phenylindole (DAPI, Sigma). Cells were imaged on a Zeiss Axiovert 2 with an ORCA-ER CCD camera (Hamamatsu) and OpenLab software (Improvision). Images were imported into Adobe Photoshop for labeling and minor alterations in contrast.
17. A-549 cells in medium with 1% fetal bovine serum were treated with DMSO vehicle ( $\leq 0.15$  % final) alone or containing compounds as specified for 18 h. To test reversibility of mitotic arrest, previously treated cells were washed three times with medium containing 1% fetal bovine serum and then replated in the same for an additional 24 h. Cells were harvested, washed twice with phosphate-buffered saline containing 2% fetal bovine serum, and then resuspended in 1 ml of the same wash buffer. For fixation, 3 ml of  $-20$  °C absolute ethanol was added slowly, followed by a 1-h incubation on ice. Fixed cells were then washed twice with phosphate-buffered saline and resuspended in staining buffer (phosphate-buffered saline containing 3.8 mM sodium citrate, 50 μg/ml propidium iodide, and 100 μg/ml RNase A) for a minimum of 1 h at 4 °C. Cells were analyzed on a BD LSR flow cytometer.
18. Vijapurkar, U.; Wang, W.; Herbst, R. *Cancer Res.* **2007**, *67*, 238.
19. Tao, W.; South, V. J.; Zhang, Y.; Davide, J. P.; Farrell, L.; Kohl, N. E.; Sepp-Lorenzino, L.; Lobell, R. B. *Cancer Cell* **2005**, *8*, 49.